Enforcing ATP hydrolysis enhanced glycolysis and promoted solvent production under anaerobic conditions

Zongjie Dai
Tianjin Institute of Industrial Biotechnology Chinese Academy of Sciences
Yan Zhu
Monash University Faculty of Medicine Nursing and Health Sciences
Hongjun Dong
University of California Berkeley
Chunhua Zhao
Institute of Microbiology Chinese Academy of Sciences
Yanping Zhang (zhangyp@im.ac.cn)
Institute of Microbiology Chinese Academy of Sciences
Yin Li
Institute of Microbiology Chinese Academy of Sciences

Research

Keywords: ATP paradox, Anaerobic fermentation, Clostridium acetobutylicum, ABE production, ATP hydrolysis

Posted Date: April 3rd, 2020

DOI: https://doi.org/10.21203/rs.3.rs-20422/v1

Abstract

Background The intracellular ATP level, an indicator of cellular energy state, plays a critical role in regulating the intracellular metabolic activities. The classical ATP paradox that the glycolytic rate negatively correlates with the intracellular ATP level was well studied. Reducing intracellular ATP level could stimulate the glycolytic rate, thereby enhancing products accumulation in aerobic conditions. However, there are limited studies about the effect of reducing cellular ATP level on anaerobic glycolysis and products formation.

Results Taking anaerobic ABE (acetone-butanol-ethanol) fermentation by Clostridium acetobutylicum as a model, we reduced the intracellular ATP level by introducing an independent ATP hydrolysis module of F 1 -ATPase. We found that the low intracellular ATP level in C. acetobutylicum compared to that in aerobic microbes, was further reduced and the glucose uptake was remarkably enhanced, achieving a 78.8% increase of volumetric glucose utilization rate. The total solvent production was improved with increase in productivity (46.5%), titer (9.9%) and yield (14.5%) compared to control, with an early onset of solventogenesis and a shortened fermentation period. Consistently, genome-scale metabolic modeling revealed the elevated metabolic fluxes through glycolysis, TCA cycle, and pyruvate metabolism in F 1 -ATPase overexpression strain.

Conclusions Decreasing the cellular energy level could further enhance the glycolytic rate at anaerobic condition and lead to significantly improvement on solvents synthesis. Our findings provide a novel strategy for improving ABE fermentation performance, which is beneficial for industrial Weizmann process. Engineering intracellular ATP level can thus be considered as a promising tool to enhance the efficiency of other anaerobic fermentation processes.

Background

The fluctuating petrol fuels supplements and associated environmental problems are motivating the development of microbial production of biofuels and chemicals from renewable feedstocks (Nielsen et al., 2013; Zhang et al., 2011). In microbial cells, glycolysis is a major metabolic route for production of biofuels and bio-chemicals (Lawford and Rousseau, 2002; Nielsen et al., 2009; Tao et al., 2001; Zhu et al., 2008). Increasing glycolysis could promote sugar utilization, elevate the overall metabolic activity and improve target product formation. Intracellular energy state (i.e. the intracellular ATP level) is known as a key factor that is able to affect the activities of rate-limiting enzymes hexose kinase, phosphofructokinase and pyruvate kinase in glycolysis pathway (Jeremy M Berg, 2002). Previous studies showed that the reduction of the intracellular ATP level could promote glycolysis and enhanced the end product formation under aerobic conditions (Causey et al., 2004; Causey et al., 2003; Chen et al., 2014; Wada et al., 2007).

For facultative aerobes, it is known from the Pasteur effect that glycolytic rate is faster under anaerobic conditions than aerobic conditions (Racker, 1974). This is mainly due to that the energy charge at

anaerobic conditions is lower, resulting from low ATP level which is only supplied by substrate phosphorylation. This phenomenon is called ATP paradox (Somsen et al., 2000), lowering the ATP level stimulates glycolytic rate, which has been verified under aerobic conditions in Escherichia coli (Koebmann et al., 2002b), Bacillus subtilis (Santana et al., 1994) and Corynebacterium glutamicum (Sekine et al., 2001). However, it is not clear the effect of further reducing energy charge on the glycolytic rate for a given obligate anaerobe. To examine this effect, we selected a model of a typical anaerobe Clostridium acetobutylicum, that performing the classic ABE fermentation, and introduced a perturbation on its energy metabolism.

Bacterial membrane-bound proton-ATPase (H^+-ATPase, EC 3.6.3.6) consists of a membrane integrated proton channel F_0 and a cytoplasmic ATP hydrolase F_1 (Dunn and Heppel, 1981; Mulkidjanian et al., 2007; Weber and Senior, 2003). To decrease intracellular ATP level, the ATP hydrolysis module F_1-ATPase was overexpressed, which could convert ATP into ADP and create an energy consumption and production loop coupled with the native ATP production reactions.

We detected the altered energy state in C. acetobutylicum after introducing an F_1-ATPase, and the effect on glycolysis as well as solvent production. Then a genome-scale metabolic model was constructed and employed to elucidate the metabolic changes in response to reduced ATP level in F_1-ATPase overexpression strain. We therefore demonstrated that manipulation the energy level can further enhance the glycolysis and products formation under anaerobic condition, which can be used as a new strategy for anaerobic fermentation.

Results And Discussion

Overexpression of F_1-ATPase reduced intracellular ATP level

To reduce the intracellular ATP level, the native F_1-ATPase genes (*atpAGD*) were cloned and expressed with plasmid $pITF_1$ in *C. acetobutylicum* DSM 1731, a model industrial strain for ABE fermentation. As expected, during the batch fermentation, the F_1-ATPase overexpression strain 1731($pITF_1$) displayed a lower ATP level compared to control strain 1731(pIMP1). The ATP level in strain 1731($pITF_1$) peaked (35μmol/gDW) at 14 hour, and rapidly declined to undetectable level thereafter; whereas the ATP level in control strain 1731(pIMP1) peaked (61 μmol/gDW) at 20 hour and remained above 40 μmol/gDW till 30 hour (**Fig 1a**). The strain 1731($pITF_1$) showed lower ATP/ADP ratio compared to that in control during the 30 hour fermentation (**Fig 1b**), indicating a significant intracellular energy depletion (Koebmann et al., 2002b). Taken together, the F_1-ATPase was functionally expressed and resulted in a significantly decreased intracellular energy state.

This strategy is very different from previous works that using the phosphoenolpyruvate synthase/pyruvate kinase ATP consuming loop for reducing intracellular ATP level (Santana et al., 1994; Sekine et al., 2001). Since this loop involved the glycolytic enzymes, it was difficult to distinguish the effects from the enzyme itself and from the changed ATP level. The independent ATP consuming module

built in this study could eliminate the uncertain effects and therefore was suitable to investigate the effect of intracellular ATP level on glycolytic rate.

Reducing cell energy state accelerated glucose utilization and promoted acidogenic growth

In aerobic metabolism, respiration is the major source of ATP production, whereas in anaerobic metabolism such as ABE fermentation of *C. acetobutylicum*, glycolysis and acidogenesis are the major source for ATP biosynthesis (Kumar et al., 2014). The effect of reduced intracellular ATP level on glycolysis and cell growth under anaerobic condition was analyzed.

Remarkably, the overexpression of the F_1-ATPase in *C. acetobutylicum* resulted in increased glucose consumption. During first 18 hour of fermentation, 290 mM glucose was consumed by strain1731(pITF$_1$), whereas only 162 mM glucose was utilized by the control strain1731(pIMP1) (**Fig2a**), representing a higher volumetric glucose utilization rate (16.15 mmol/L/h) in 1731(pITF$_1$) compared to 9.03 mmol/L/h in control at acidogenesis phase. As to specific glucose utilization rate, two strains had similar maximal specific rate, but strain DSM 1731(pITF$_1$) had great advantage to control strain during the first 18 hours (**Fig 2b**).

Oxidative phosphorylation and substrate level phosphorylation are the two types of phosphorylation for ATP formation in living organism. One molecule of glucose oxidized by aerobic respiration generates more ATPs than anaerobic fermentation, this absolute ATP level difference determines that the glycolytic rate is higher in anaerobic condition than aerobic condition. Interestingly, the glucose utilization rate was further increased in anaerobic *C. acetobutylicum* by lowering the ATP level. Although the glycolytic rate of *E. coli* were also increased under anaerobic condition by introducing the phosphoenolpyruvate synthase/pyruvate kinase substrate futile cycle (Hadicke et al., 2015). However, this work can't differentiate the causality between ATP level and expression of these glycolytic involved enzymes. For the first time we confirmed that reducing ATP level could increase glycolytic rate at obligate anaerobic growing condition considering no increase in glycolytic flux in steadily growing *Lactococcus lactis* cells (Koebmann et al., 2002a). This work indicated that the relative ATP level changes controlled the glycolytic rate irrespective of aerobic or anaerobic conditions. It also showed the universality of the ATP paradox which was firstly found in eukaryal *Saccharomyces cerevisiae* (Larsson et al., 1997; Somsen et al., 2000).

The specific growth rate of DSM 1731(pITF$_1$) was also higher than that of DSM 1731(pIMP1) during first 18 hours, although the maximal specific growth rate was little lower (**Fig 2c**). As to aerobic and facultative aerobic bacteria, the slower growth rate was reported in the lower ATP level cells (Koebmann et al., 2002b; Rud et al., 2008), which was also approved in this work through obligate anaerobic *C. acetobutylicum* with the lower maximal specific growth rate. However, compared to the control strain, higher growth rates were achieved by the lower ATP level strain1731(pITF$_1$) in the first 18 hour, which might due to the unique two stages (acido- and solventogenesis) fermentation of *C. acetobutylicum* whose cell growth may be inhibited by the acids accumulation in acidogenesis stage. As a result, the peak value of OD_{600} was 17.2 in strain 1731(pITF$_1$) versus 13.9 in 1731(pIMP1), representing a 22.8%

increment (**Fig 2d**). This is the highest optical density in *C. acetobutylicum* during batch fermentation compared with previous works (Harris et al., 2001; Mao et al., 2009; Zhu et al., 2011). Low cell density fermentation is a disadvantage of clostridia compared with other industrial strains, such as yeast and lactobacillus. As to solventogenic clostridia, high cell density fermentation is necessary to develop effective continuous butanol production with better volumetric productivity (Nguyen et al., 2018).

Reduced cell energy state decreased acid accumulation and enhanced solvent production

The fermentation of *C. acetobutylicum* is featured by two distinct stages, i.e. acidogenesis and solventogenesis (Jones et al., 2008). Reduced intracellular energy state altered these two stages fermentation profiles in *C. acetobutylicum*. Strain1731(pITF$_1$) produced 33.8% less total acids and 9.9% more total solvents (**Fig 3**).

The maximum production of acetate and butyrate were 11.4 mM and 33.5 mM in strain 1731(pITF$_1$), representing 54.4% and 33.5% decrease compared to control. The final residual acetate and butyrate of strain 1731(pITF$_1$) also lower than the control (**Fig 3a and 3b**). It indicated that stronger acid re-assimilation occurred in F$_1$-ATPase overexpressing strain. Butyrate and/or acetate was thought as the inhibition factor to low cell density for solventogenic clostridia (Papoutsakis, 2008). Lower acetate and butyrate concentration caused by reduced cell energy state may be a reason why 1731(pITF$_1$) had higher cell density.

In the other hand, the highest concentrations of butanol, acetone and ethanol in strain 1731(pITF$_1$) reached 194.9, 83.6 and 51.4 mM respectively, representing 3.3%, 22.5% and 33.6% increases compared to the control strain (**Fig 3a and 3b**). The total solvent yield was also increased by 14.5%, reached 31.8% in strain 1731(pITF$_1$). In addition, the fermentation period was shortened, strain 1731(pITF$_1$) needs only 30 hour to achieve the maximal solvent titer, which is at least 10 hour less compared with control (**Fig 3a and 3b**). Thus the maximal solvent productivity of strain 1731(pITF$_1$) solvents was significantly improved, representing 46.5% increases compared with the control.

Low ATP levels triggered the early onset of solventogenesis

The effect of cellular energy state on the switch from acidogenesis to solventogenesis was controversial. Some researchers thought that the decreased ATP concentration and corresponding increased ADP concentration was assumed as an internal signal for the shift from acidogenesis to solventogenesis in continuous culture (Grupe and Gottschalk, 1992). Some others proposed an opposite hypothesis that ATP limitation would be associated with acidogenesis, while high ATP concentrations are related to solventogenesis in continuous cultures (Meyer and Papoutsakis, 1989a). However, the others suggested ATP level appeared to no correlation with normal solventogenesis in batch cultures (Meyer and Papoutsakis, 1989b).

In this study strain 1731(pITF$_1$) started to re-utilize acids for producing solvents around 10 hours earlier than control (**Fig 3**), indicating the earlier initiation of the solventogenic phase. Real-time determination of extracellular pH and oxidoreductive potential (ORP) further validated this conclusion (**Fig 4**). The culture pH of 1731(pITF$_1$) dropped down to the threshold 5.0 because of acids accumulation, and rose back much earlier and faster compared to control, which indicated the advanced acids re-assimilation (**Fig 4a**). The culture ORP reflects the total oxidative or reductive properties of the fermentation broth (Zhu et al., 2014). Solvent production would increase the reductive property of the medium and led to the decline of ORP value. In the beginning, the ORP level of overexpression strain remained stable and similar as that of control, but quickly dropped to its lowest value after 12 h whereas the ORP level of control strain slowly declined to its lowest value at 30 h, suggesting the earlier initiation of solvents production (**Fig 4b**). These results indicated that the transition from acidogenesis to solventogenesis was brought forward by reducing intracellular ATP level during glucose batch fermentation.

The possible reason is that the increased glycolytic rate caused by reduced ATP concentration would lead to more NADH formation. This hypothesis was supported by determining the intracellular NADH and NAD^+ levels and calculating NADH turnover rate. Though the NADH/NAD ratio of the two strains were similar, the NADH turnover rate of strain DSM1731(pITF$_1$) was much higher compared to the control strain in first 18 hour of fermentation (**Fig 4c and 4d**). High NADH availability was supposed to lead to solventogenesis (Grupe and Gottschalk, 1992). Alcohol production as one of outlets of NADH in *C. acetobutylicum*, the balance between NADH production and its oxidation could be a driving force to induce the strain to produce alcohol earlier and stronger. This is approved by the 213.5% and 103.8% increment for butanol and ethanol production in energy reduced strain compared with control strain at 18 hour. These might explain why reduced cell energy state led to advanced solventogenesis.

Cellular metabolic change induced by depleted intracellular ATPs

The intracellular ATP level allosterically regulates many metabolic enzymes (Jeremy M Berg, 2002), and the depletion of intracellular ATP by overexpression of F_1-ATPase could result in significant metabolic flux changes at network level. A genome-scale metabolic model (*i*DSM1731) was constructed for *C. acetobutylicum* DSM 1731 using the genome annotation and literature. The model contained 766 genes, 775 metabolites and 1,003 reactions, and it was used to calculate the metabolic fluxes in strains 1731(pITF$_1$) and 1731(pIMP1) during batch fermentation.

In F_1-ATPase overexpression strain 1731(pITF$_1$), the glycolytic fluxes were enhanced in acidogenesis phase compared to control strain 1731(pIMP1), and then dramatically declined after 12 hour (**Fig 5a**). In glycolysis, phosphofructokinase (PFK) and pyruvate kinase (PYK) are two key enzymes allosterically regulation by the intracellular ATP level (Jeremy M Berg, 2002). The reduced ATP level in 1731(pITF$_1$) could alleviate the allosteric inhibition, enhance the activity of PFK and PYK, and increase the overall glycolytic fluxes. Model simulation showed an increased flux through pyruvate ferredoxin oxidoreductase (POR) and an enhanced hydrogen production via hydrogenase (FDXNH) in acidogenic phase (**Fig 5a**) in

1731(pITF$_1$) compared to 1731(pIMP1). Hydrogen formation utilizes the redox power from NADH and thus is an important path for oxidation of excess NADH in acidogenesis (Jones et al., 2008). Along with enhanced hydrogen production, sufficient NAD^+ was generated for use in enhanced glycolysis in 1731(pITF$_1$). Furthermore, compared to control strain 1731(pIMP1), in F_1-ATPaseoverexpression strain 1731(pITF$_1$) the tricarboxylic acid cycle (TCA) fluxes (e.g. citrate synthase [CS], aconitase [ACON], isocitrate dehydrogenase [IDH]) were higher at 6 hour of fermentation (**Fig 5b**), but remained at a low level thereafter. Together, the enhanced metabolic activity in glycolysis and TCA could produce ample energy and building blocks (e.g. amino acids, nucleotides and lipids) for increased growth in 1731(pITF$_1$) as shown above (**Fig 1c**).

Within ABE fermentation pathways, the flux through thiolase (ACACT) was 2.3-fold higher (3.7 mM/gDW/h versus1.1mM/gDW/h) in strain 1731(pITF$_1$) than that in control at 12 hour, but remarkably lower at the following time points, thereby generating an enhanced flux towards butyryl-CoA, the precursor of butanol production. In F_1-ATPase overexpression strain 1731(pITF$_1$), the fluxes through solventogenic enzymes (e.g. acetoacetate decarboxylase [ADC], CoA transferase [COAT1/COAT2], alcohol dehydrogenase [ALCD/BUTOH]) were significantly induced at 12 hour, whereas they were induced at 18 hour in control strain 1731(pIMP1) (**Fig 5c**).These results also indicate an early onset of solventogenesis owing to depletion of intracellular ATP.

Conclusions

Decreased cell energy state was first time realized by creating an independent ATP hydrolysis module in obligate anaerobe Clostridium. At anaerobic condition, glycolytic rate was further increased by the reduced ATP level. The upregulated metabolic flux through glycolysis, TCA cycle, pyruvate and amino acid metabolism ensured the better cell growth. In addition, stronger solvent productivity and higher solvent titer and yield were achieved in this work. And the solventogenesis was brought forward by reducing cell energy state. Our study indicated that even in anaerobic condition decreasing cell energy state could still increase the glycolytic flux and promote products accumulation. This work confirmed that ATP paradox was also adaptable in obligate anaerobes and anaerobic conditions. It indicated a new strategy for engineering anaerobic fermentation.

Materials And Methods

Bacterial strains and culture conditions. *C. acetobutylicum* strain DSM 1731 and its derivatives (Table S1) were grown in Reinforced Clostridial Medium (RCM) anaerobically at 37°C (Dong et al., 2010; Wang et al., 2011). All *E. coli* strains were grown aerobically in Luria-Bertani (LB) broth at 37°C with vigorous shaking at 220 rpm (Hirsch and Grinsted, 1954). *E. coli* JM109 was employed for gene cloning. Shuttle vector was methylated by transforming *E. coli* ER2275 bearing methylating plasmid pAN1. Ampicillin (100 μg/ml) and erythromycin (50 μg/ml) were used for screening and maintaining of plasmids, when necessary. Cell

growth was monitored by measuring the optical density at 600 nm (OD_{600}) with a UV/Vis 2802PC spectrophotometer (Unico, New Jersey, USA).

Overexpression of F_1-ATPase in DSM 1731. The F_1 component encoding genes, *atpAGD* (SMB_G2901-SMB_G2903), and thiolase promoter (P_{thl}) were amplified from DSM1731 genome using primers atpAGD-1: 5'-CGCGGATCCATGAACATAAAACCTGAAGAGATAACTTCA-3', atpAGD-2: 5'-CCGGAATTCTTAGCTTTCCATCATTTTTTTAGCTTT-3', thl-1: 5'-CGCGTCGACTATATTGATAAAAATAATAATAGTG and thl-2: 3'-CGCGGATCCTTCTTTCATTCTAACTAACCTCCTA. The fragments were then jointed and cloned into the shuttle vector pIMP1 (Mermelstein et al., 1992). The derived plasmid was designated as $pITF_1$. Insertion of DNA sequence was confirmed by sequencing. pIMP1 and $pITF_1$ (Table S1) were methylated before transformation of DSM1731 (Mermelstein and Papoutsakis, 1993). Electroporation to DSM1731 was performed based on previous protocol.

Batch fermentation. Batch fermentation were performed in two 7.5-L BioFlo 110 fermentors (New Brunswick Scientific, Edison, NJ) containing 3.0 L clostridium growth medium (CGM) (Dai et al., 2016; Wiesenborn et al., 1988). Anaerobic conditions were assured by continuously sparging nitrogen into reactor. Refined corn oil (2.7 ml/L) was added for defoaming purpose. The reactor medium (initial pH 7.0) was inoculated with 300-ml preculture of early log-phase (OD_{600}~2.0). Broth pH was monitored by pH meter (Mettler-Toledo) and controlled above 5.0 by adding 6 M ammonia automatically. Broth oxidoreductive potential (ORP) was measured by on-line ORP electrode (Mettler-Toledo). Extracellular metabolites including glucose, butanol, ethanol, acetone, butyrate and acetate were determined by high performance liquid chromatography (Agilent Technologies, Santa Clara, CA).

Quantification of intracellular ATP, ADP, NADH and NAD^+. Intracellular ATP and ADP were extracted with perchloric acid method as described previously (Cole et al., 1967) with minor modifications. Samples were collected at multiple time points and subjected to centrifugation at 10,000 × g for 1 min. The cell pellets were homogenized immediately in 200 µl ice-cold 7% perchloric acid and incubated on ice for 10 min. After centrifugation at 15,000 × g for 5 min, the supernatant was collected and neutralized using 50 µl 3 M potassium hydroxide, 100 µl 0.4 M Tris, 50 µl 3 M potassium chloride. The mixture was vortexed thoroughly and subjected to another centrifugation at 15,000 × g for 5 min to remove any residual precipitate. Then the supernatant was transferred to another sterile centrifuge tube for HPLC analysis. An ion-pair reversed-phase HPLC method was used to determine the intracellular adenine nucleotides level according to previous work (Napolitano and Shain, 2005; Zur Nedden et al., 2009) with optimization. Agilent 1200 HPLC was used with 10 µl injection each time. The mobile phase consisted of potassium phosphate dibasic (107.5 mM), tetrabutylammonium hydrogen sulphate (2.3 mM) and acetonitrile (6%) at pH 6.25 was pumped through a C18 column (SB-AQ 4.6×250 mm, 5-micron, Agilent) at a flow rate of 1 ml/min.

The extraction and determination of intracellular NADH and NAD^+ was conducted as preciously described (Menzel et al., 1998) with only slight modifications. To prepare NADH, 400 µlice-cold 0.4 M potassium

hydroxide was firstly added into 1 ml fermentation broth. The mixture was then incubated at 30^{o}Cfor 10 min and subject to a centrifugation at 15,000 × g for 10 min at 4^{o}C. Approximate 200 µl supernatant was collected and neutralized to pH 7.5-8.0 by adding 0.4 M hydrochloride acid. For NAD^+, 400 µl ice-cold 0.4 M hydrochloride acid was added to 1 ml broth. The mixture was incubated at 50^{o}Cfor 10 min and centrifuged at 15,000 × g for 10 min at 4^{o}C. Approximate 200 µl supernatant was collected and neutralized to pH 7.2-7.4 by using 0.4 M potassium hydroxide. The neutralized samples were immediately used for NADH and NAD^+ determination. The spectrometric enzymatic cycling assay was applied with slight modifications. The assay mixture contained 2 ml buffer (0.15 M glycylglycine/nicotinic acid buffer, pH 7.4), 400 µl phenanziniummethylsulfate (PES) (4 mg/ml), 400 µl thiazolyl-blue (MTT) (5 mg/ml), 70 µl ethanol and 40 µl alcohol dehydrogenase (60 U/ml). After addition of 50 µl neutralized sample into reaction buffer and a brief vortexing, absorption was examined by using spectrophotometer for 10 min at 570 nm.

GSMM construction for *C. acetobutylicum* DSM 1731. The model construction started with collecting genome annotation and metabolic and transport reactions from KEGG (Kanehisa et al., 2017) and BioCyc (Caspi et al., 2016). The genome annotation of strain DSM 1731 (Accession No. GCA_000218855.1) was obtained from GenBank database. A draft model was constructed based on the predicted metabolic functions in KEGG, and then supplemented with the missing metabolites, reactions and genes according to the genome annotation of DSM 1731 and BioCyc. Extensive manual curation was conducted to improve the model, including (i) adding extracellular metabolites, (ii) adding exchange and transport reactions, (ii) filling pathway gaps, and (iii) checking the mass and charge balance of each reaction. The resulting model was compiled in Systems Biology Markup Language (Hucka et al., 2015). VANTED (Rohn et al., 2012) was employed for metabolic network visualization and analysis. The biomass formation equation consisting of necessary building blocks for growth was created using the one from existing model for ATCC 824 model owing to its very close phylogeny relationship to this type strain. The minimum of non-growth associated maintenance (NGAM) was set to 2 mmol/gDW/h according to previous modeling effort (Lee et al., 2008).

Constraints-based metabolic modeling. The batch fermentation data above were employed to estimate the specific rates including (i) specific growth rate μ, (ii) specific glucose uptake $r_{glc,}$ and (iii) secretion rates of acetate (r_{ac}), butyrate (r_{but}), acetone (r_{act}), ethanol (r_{etoh}) and butanol (r_{butol}) for both wild type and F_1-ATPase overexpression strains, using B-spline smoothing algorithm (Oner et al., 1986). At each time point (i.e. 6, 12, 18, 24 h), the calculated specific rates were used to constrain the corresponding exchange fluxes in *i*DSM1731 with up to 5% variations. The optimal specific growth rate (μ^*) was firstly calculated using flux balance analysis with the imposed constrains above. Then the solution spaces of the constrained GSMM were sampled with 1,000 points using artificially centered hit-and-run (ACHR) algorithm (Kaufman and Smith, 1998) with the specific growth rate set to ≥ 99% μ^*. The obtained feasible solutions were adjusted by applying loopless COBRA (ll-COBRA) method (Schellenberger et al., 2011) to avoid unnecessary flux loops. Student's *t*-test was conducted to determine the differentially changed metabolic fluxes with FDR (false discovery rate) adjusted $P < 0.05$. Metabolite turnover rates

were calculated by summing up all the incoming or outgoing fluxes around the metabolite (Chung and Lee, 2009) using equation $\varphi = \sum_j s_{ij} v_j$.

Abbreviations

ABE, acetone-butanol-ethanol; CGM, clostridial growth medium; RCM, reinforced clostridial medium; HPLC, high performance liquid chromatography; GC-MS, gas chromatography-mass spectrometry; RI, refractive index; TE, tris-ethylenediaminetetraacetic acid; SDS-PAGE, sodium dodecyl sulfate polyacrylamide gel electrophoresis; ORP, oxidoreductive potential; PES, phenanzinium methylsulfate; MTT, thiazolyl-blue; NGAM, non-growth associated maintenance; ACHR, artificially centered hit-and-run; GSMM, genome-scale metabolic modeling.

Declarations

Ethics approval and consent to participate

Not applicable.

Consent for publication

All authors consent for publication.

Competing interests

The authors declare that they have no conflict of interests.

Funding

This work was supported by grants from the National Natural Science Foundation of China (31870038, 31670048), the National High Technology Research and Development Program of China (2011AA02A208), and the Science and Technology Service Network Initiative of Chinese Academy of Sciences (STS project). Yanping Zhang was supported by the Youth Innovation Promotion Association of the Chinese Academy of Sciences (2014076).

Authors' contributions

Conceived the experiments: ZJD, YL, HJD and YPZ. Performed the experiments: ZJD and HJD. Analyzed the data: ZJD and YZ. Contributed reagents/materials/analysis tools: ZJD, HJD and YZ. Wrote the paper: ZJD, YZ, CHZ, YPZ and YL.

Acknowledgements

The authors are indebted to Professor Eleftherios Terry Papoutsakis (University of Delaware, USA) for his kind providing pIMP1 and *E. coli* ER2275(pAN1).

Availability of data and materials

All data generated or analyzed in the present study are included in this article and in additional information.

References

Caspi, R., Billington, R., Ferrer, L., Foerster, H., Fulcher, C. A., Keseler, I. M., Kothari, A., Krummenacker, M., Latendresse, M., Mueller, L. A., Ong, Q., Paley, S., Subhraveti, P., Weaver, D. S., Karp, P. D., 2016. The MetaCyc database of metabolic pathways and enzymes and the BioCyc collection of pathway/genome databases. Nucleic Acids Res. 44, pp. D471-D480.

Causey, T. B., Shanmugam, K. T., Yomano, L. P., Ingram, L. O., 2004. Engineering *Escherichia coli* for efficient conversion of glucose to pyruvate. Proc. Natl. Acad. Sci. U. S. A. 101, pp. 2235-2240.

Causey, T. B., Zhou, S., Shanmugam, K. T., Ingram, L. O., 2003. Engineering the metabolism of *Escherichia coli* W3110 for the conversion of sugar to redox-neutral and oxidized products: Homoacetate production. Proc. Natl. Acad. Sci. U. S. A. 100, pp. 825-832.

Chen, Y., Liu, Q. G., Chen, X. C., Wu, J. L., Xie, J. J., Guo, T., Zhu, C. J., Ying, H. J., 2014. Control of glycolytic flux in directed biosynthesis of uridine-phosphoryl compounds through the manipulation of ATP availability. Appl. Microbiol. Biotechnol. 98, pp. 6621-6632.

Chung, B. K., Lee, D. Y., 2009. Flux-sum analysis: a metabolite-centric approach for understanding the metabolic network. BMC Syst. Biol. 3, p. 117.

Cole, H. A., Wimpenny, J. W., Hughes, D. E., 1967. The ATP pool in *Escherichia coli*. I. Measurement of the pool using modified luciferase assay. Biochim. Biophys. Acta. 143, pp. 445-453.

Dai, Z., Dong, H., Zhang, Y., Li, Y., 2016. Elucidating the contributions of multiple aldehyde/alcohol dehydrogenases to butanol and ethanol production in *Clostridium acetobutylicum*. Sci. Rep. 6, p. 28189.

Dong, H. J., Zhang, Y. P., Dai, Z. J., Li, Y., 2010. Engineering *Clostridium* strain to accept unmethylated DNA. PLoS One. 5, p. e9038.

Dunn, S. D., Heppel, L. A., 1981. Properties and functions of the subunits of the *Escherichia coli* coupling factor ATPase. Arch. Biochem. Biophys. 210, pp. 421-436.

Grupe, H., Gottschalk, G., 1992. Physiological events in *Clostridium acetobutylicum* during the shift from acidogenesis to solventogenesis in continuous culture and presentation of a model for shift induction. Appl. Environ. Microbiol. 58, pp. 3896-3902.

Hadicke, O., Bettenbrock, K., Klamt, S., 2015. Enforced ATP futile cycling increases specific productivity and yield of anaerobic lactate production in *Escherichia coli*. Biotechnol. Bioeng. 112, pp. 2195-2199.

Harris, L. M., Blank, L., Desai, R. P., Welker, N. E., Papoutsakis, E. T., 2001. Fermentation characterization and flux analysis of recombinant strains of *Clostridium acetobutylicum* with an inactivated *solR* gene. J. Ind. Microbiol. Biotechnol. 27**,** pp. 322-328.

Hirsch, A., Grinsted, E., 1954. Methods for the growth and enumeration of anaerobic spore-formers from cheese, with observations on the effect of nisin. J. Dairy Res. 21**,** pp. 101-110.

Hucka, M., Bergmann, F. T., Drager, A., Hoops, S., Keating, S. M., Le Novere, N., Myers, C. J., Olivier, B. G., Sahle, S., Schaff, J. C., Smith, L. P., Waltemath, D., Wilkinson, D. J., 2015. Systems biology markup language (SBML) level 2 version 5: structures and facilities for nodel definitions. J. Integr. Bioinform. 12**,** p. 271.

Jeremy M Berg, John L Tymoczko, Lubert Stryer, 2002. The glycolytic pathway is tightly controlled. Biochemistry. W H Freeman, New York.

Jones, S.W., Paredes, C.J., Tracy, B., Cheng, N., Sillers, R., Senger, R.S., Papoutsakis, E.T., 2008. The transcriptional program underlying the physiology of clostridial sporulation. Genome Biol. 9**,** p. R114.

Kanehisa, M., Furumichi, M., Tanabe, M., Sato, Y., Morishima, K., 2017. KEGG: new perspectives on genomes, pathways, diseases and drugs. Nucleic Acids Res. 45**,** pp. D353-D361.

Kaufman, D. E., Smith, R. L., 1998. Direction choice for accelerated convergence in hit-and-run sampling. Oper. Res. 46**,** pp. 84-95.

Koebmann, B. J., Solem, C., Pedersen, M. B., Nilsson, D., Jensen, P. R., 2002a. Expression of genes encoding F_1-ATPase results in uncoupling of glycolysis from biomass production in *Lactococcus lactis*. Appl. Environ. Microbiol. 68**,** 4274-4282.

Koebmann, B. J., Westerhoff, H. V., Snoep, J. L., Nilsson, D., Jensen, P. R., 2002b. The glycolytic flux in *Escherichia coli* is controlled by the demand for ATP. J. Bacteriol. . 184**,** pp. 3909-3916.

Kumar, M., Saini, S., Gayen, K., 2014. Elementary mode analysis reveals that *Clostridium acetobutylicum* modulates its metabolic strategy under external stress. Mol. Biosyst. 10**,** pp. 2090-2105.

Larsson, C., Nilsson, A., Blomberg, A., Gustafsson, L., 1997. Glycolytic flux is conditionally correlated with ATP concentration in *Saccharomyces cerevisiae*: a chemostat study under carbon- or nitrogen-limiting conditions. J. Bacteriol. 179**,** pp. 7243-7250.

Lawford, H. G., Rousseau, J. D., 2002. Steady-state measurements of lactic acid production in a wild-type and a putative D-lactic acid dehydrogenase-negative mutant of *Zymomonas mobilis*: influence of glycolytic flux. Appl. Biochem. Biotechnol. 98-100**,** pp. 215-228.

Lee, J., Yun, H., Feist, A. M., Palsson, B. O., Lee, S. Y., 2008. Genome-scale reconstruction and in silico analysis of the *Clostridium acetobutylicum* ATCC 824 metabolic network. Appl. Microbiol. Biotechnol. 80**,**

pp. 849-862.

Mao, S., Luo, Y., Zhang, T., Li, J., Bao, G., Zhu, Y., Chen, Z., Zhang, Y., Li, Y., Ma, Y., 2009. Proteome reference map and comparative proteomic analysis between a wild type *Clostridium acetobutylicum* DSM 1731 and its mutant with enhanced butanol tolerance and butanol yield. J. Proteome Res. 9**,** pp. 3046-3061.

Menzel, K., Ahrens, K., Zeng, A., Deckwer, W., 1998. Kinetic, dynamic, and pathway studies of glycerol metabolism by *Klebsiella pneumoniae* in anaerobic continuous culture: IV. Enzymes and fluxes of pyruvate metabolism. Biotechnol. Bioeng. 60**,** pp. 617-626.

Mermelstein, L. D, Welker, N. E, Bennett, G. N, Papoutsakis, E. T, 1992. Expression of cloned homologous fermentative genes in *Clostridium acetobutylicum* ATCC 824. Nat. Biotechnol. 10**,** pp. 190-195.

Mermelstein, L. D., Papoutsakis, E. T., 1993. *In vivo* methylation in *Escherichia coli* by the *Bacillus subtilis* phage phi 3T I methyltransferase to protect plasmids from restriction upon transformation of *Clostridium acetobutylicum* ATCC 824. Appl. Environ. Microbiol. 59**,** pp. 1077-1081.

Meyer, C. L., Papoutsakis, E. T., 1989a. Continuous and biomass recycle fermentations of *Clostridium acetobutylicum* .1. ATP supply and demand determines product selectivity. Bioprocess. Eng. . 4**,** pp. 1-10.

Meyer, C. L., Papoutsakis, E. T., 1989b. Increased Levels of ATP and NADH are associated with increased solvent production in continuous cultures of *Clostridium acetobutylicum*. Appl. Microbiol. Biotechnol. . 30**,** pp. 450-459.

Mulkidjanian, A. Y., Makarova, K. S., Galperin, M. Y., Koonin, E. V., 2007. Inventing the dynamo machine: the evolution of the F-type and V-type ATPases. Nat. Rev. Microbiol. 5**,** pp. 892-899.

Napolitano, M. J., Shain, D. H., 2005. Quantitating adenylate nucleotides in diverse organisms. J. Biochem. Bioph. Methods 63**,** pp. 69-77.

Nguyen, N. P., Raynaud, C., Meynial-Salles, I., Soucaille, P., 2018. Reviving the Weizmann process for commercial n-butanol production. Nat. Commun. 9**,** p. 3682.

Nielsen, D. R., Leonard, E., Yoon, S. H., Tseng, H. C., Yuan, C., Prather, K. L., 2009. Engineering alternative butanol production platforms in heterologous bacteria. Metab. Eng. 11**,** pp. 262-273.

Nielsen, J., Larsson, C., van Maris, A., Pronk, J., 2013. Metabolic engineering of yeast for production of fuels and chemicals. Curr. Opin. Biotechnol. 24**,** pp. 398-404.

Oner, M. D., Erickson, L. E., Yang, S. S., 1986. Utilization of spline functions for smoothing fermentation data and for estimation of specific rates. Biotechnol. Bioeng. 28**,** pp. 902-918.

Papoutsakis, E. T., 2008. Engineering solventogenic clostridia. Curr. Opin. Biotechnol. 19**,** pp. 420-429.

Racker, E., 1974. History of the Pasteur effect and its pathobiology. Mol. Cell. Biochem. 5**,** pp. 17-23.

Rohn, H., Junker, A., Hartmann, A., Grafahrend-Belau, E., Treutler, H., Klapperstuck, M., Czauderna, T., Klukas, C., Schreiber, F., 2012. VANTED v2: a framework for systems biology applications. BMC Syst. Biol. 6**,** p. 139.

Rud, I., Solem, C., Jensen, P. R., Axelsson, L., Naterstad, K., 2008. Co-factor engineering in lactobacilli: Effects of uncoupled ATPase activity on metabolic fluxes in *Lactobacillus (L.) plantarum* and *L. sakei*. Metab. Eng. 10**,** pp. 207-215.

Santana, M., Ionescu, M. S., Vertes, A., Longin, R., Kunst, F., Danchin, A., Glaser, P., 1994. *Bacillus subtilis* F_0F_1-ATPase: DNA sequence of the atp operon and characterization of atp mutants. J. Bacteriol. 176**,** pp. 6802-6811.

Schellenberger, J., Que, R., Fleming, R. M., Thiele, I., Orth, J. D., Feist, A. M., Zielinski, D. C., Bordbar, A., Lewis, N. E., Rahmanian, S., Kang, J., Hyduke, D. R., Palsson, B. O., 2011. Quantitative prediction of cellular metabolism with constraint-based models: the COBRA Toolbox v2.0. Nat. Protoc. 6**,** pp. 1290-1307.

Sekine, H., Shimada, T., Hayashi, C., Ishiguro, A., Tomita, F., Yokota, A., 2001. H^+-ATPase defect in *Corynebacterium glutamicum* abolishes glutamic acid production with enhancement of glucose consumption rate. Appl. Microbiol. Biotechnol. 57**,** pp. 534-540.

Somsen, OJ, Hoeben, M.A., Esgalhado, E., Snoep, J.L., Visser, D., Van Der Heijden, RT, Heijnen, JJ, Westerhoff, HV, 2000. Glucose and the ATP paradox in yeast. Biochem. J. 352**,** p. 593.

Tao, H., Gonzalez, R., Martinez, A., Rodriguez, M., Ingram, L. O., Preston, J. F., Shanmugam, K. T., 2001. Engineering a homo-ethanol pathway in *Escherichia coli*: increased glycolytic flux and levels of expression of glycolytic genes during xylose fermentation. J. Bacteriol. 183**,** pp. 2979-2988.

Wada, M., Narita, K., Yokota, A., 2007. Alanine production in an H+-ATPase- and lactate dehydrogenase-defective mutant of *Escherichia coli* expressing alanine dehydrogenase. Appl. Microbiol. Biotechnol. 76**,** pp. 819-825.

Wang, S., Zhang, Y., Dong, H., Mao, S., Zhu, Y., Wang, R., Luan, G., Li, Y., 2011. Formic acid triggers the "Acid Crash" of acetone-butanol-ethanol fermentation by *Clostridium acetobutylicum*. Appl. Environ. Microbiol. 77**,** pp. 1674-1680.

Weber, J., Senior, A. E., 2003. ATP synthesis driven by proton transport in F_1F_0-ATP synthase. FEBS Lett. 545**,** pp. 61-70.

Wiesenborn, D. P., Rudolph, F. B., Papoutsakis, E. T., 1988. Thiolase from *Clostridium acetobutylicum* ATCC 824 and its role in the synthesis of acids and solvents. Appl. Environ. Microbiol. 54**,** pp. 2717-2722.

Zhang, F., Rodriguez, S., Keasling, J. D., 2011. Metabolic engineering of microbial pathways for advanced biofuels production. Curr. Opin. Biotechnol. 22**,** pp. 775-783.

Zhu, L. J., Dong, H. J., Zhang, Y. P., Li, Y., 2011. Engineering the robustness of *Clostridium acetobutylicum* by introducing glutathione biosynthetic capability. Metab. Eng. 13**,** pp. 426-434.

Zhu, Y., Eiteman, M. A., Altman, R., Altman, E., 2008. High glycolytic flux improves pyruvate production by a metabolically engineered *Escherichia coli* strain. Appl. Environ. Microbiol. 74**,** pp. 6649-6655.

Zhu, Y., Li, D., Bao, G. H., Wang, S. H., Mao, S. M., Song, J. N., Li, Y., Zhang, Y. P., 2014. Metabolic changes in *Klebsiella* oxytoca in response to low oxidoreduction potential, as revealed by comparative proteomic profiling integrated with flux balance analysis. Appl. Environ. Microbiol. 80**,** pp. 2833-2841.

Zur Nedden, S., Eason, R., Doney, A. S., Frenguelli, B. G., 2009. An ion-pair reversed-phase HPLC method for determination of fresh tissue adenine nucleotides avoiding freeze-thaw degradation of ATP. Anal. Biochem. 388**,** pp. 108-114.

Figures

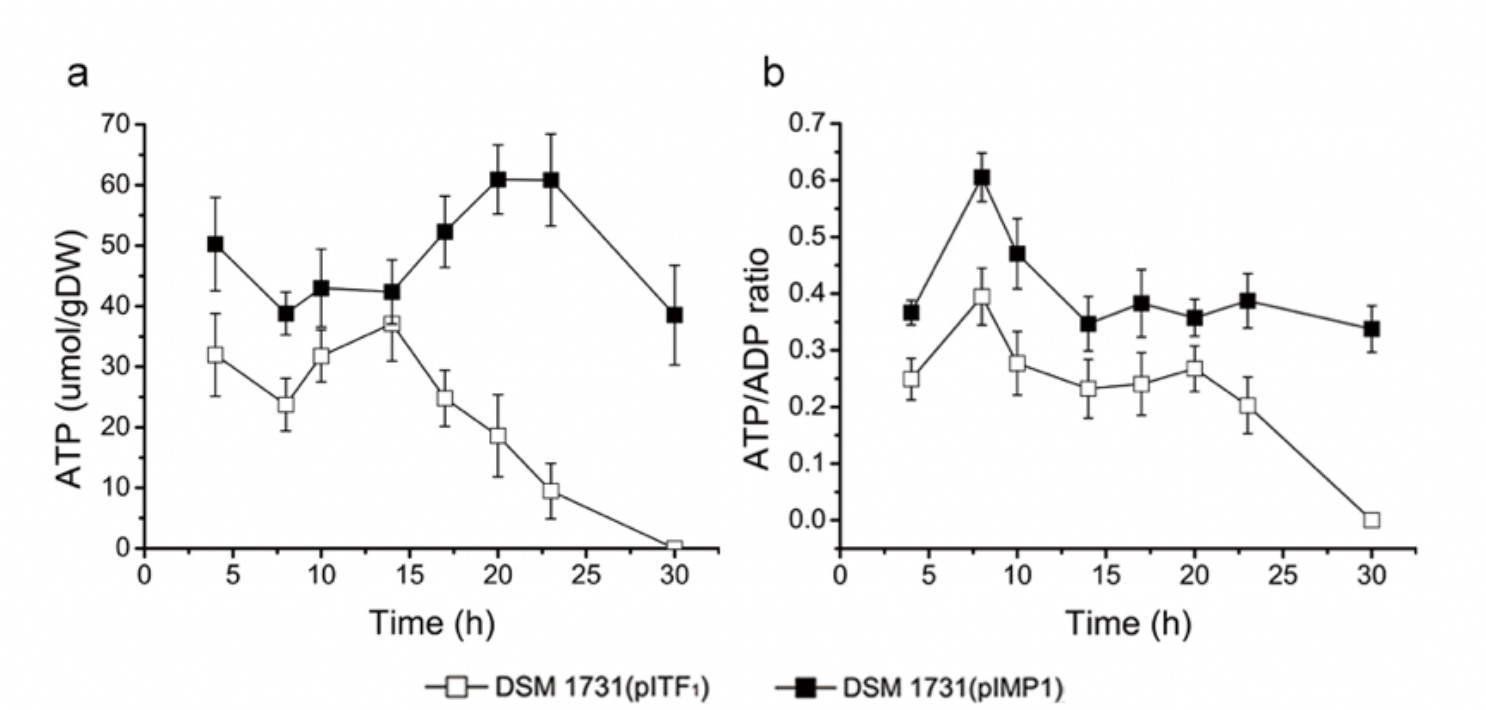

Figure 1

Effect of overexpression of F1-ATPase on intracellular energy level in C. acetobutylicum DSM1731. (a) The ATP concentration of two strains. These results were created by three repeat experiments. (b) The ATP/ADP ratio of strain DSM1731(pITF1) and control strain DSM1731(pIMP1) during the prior 30 hours of the whole fermentation period.

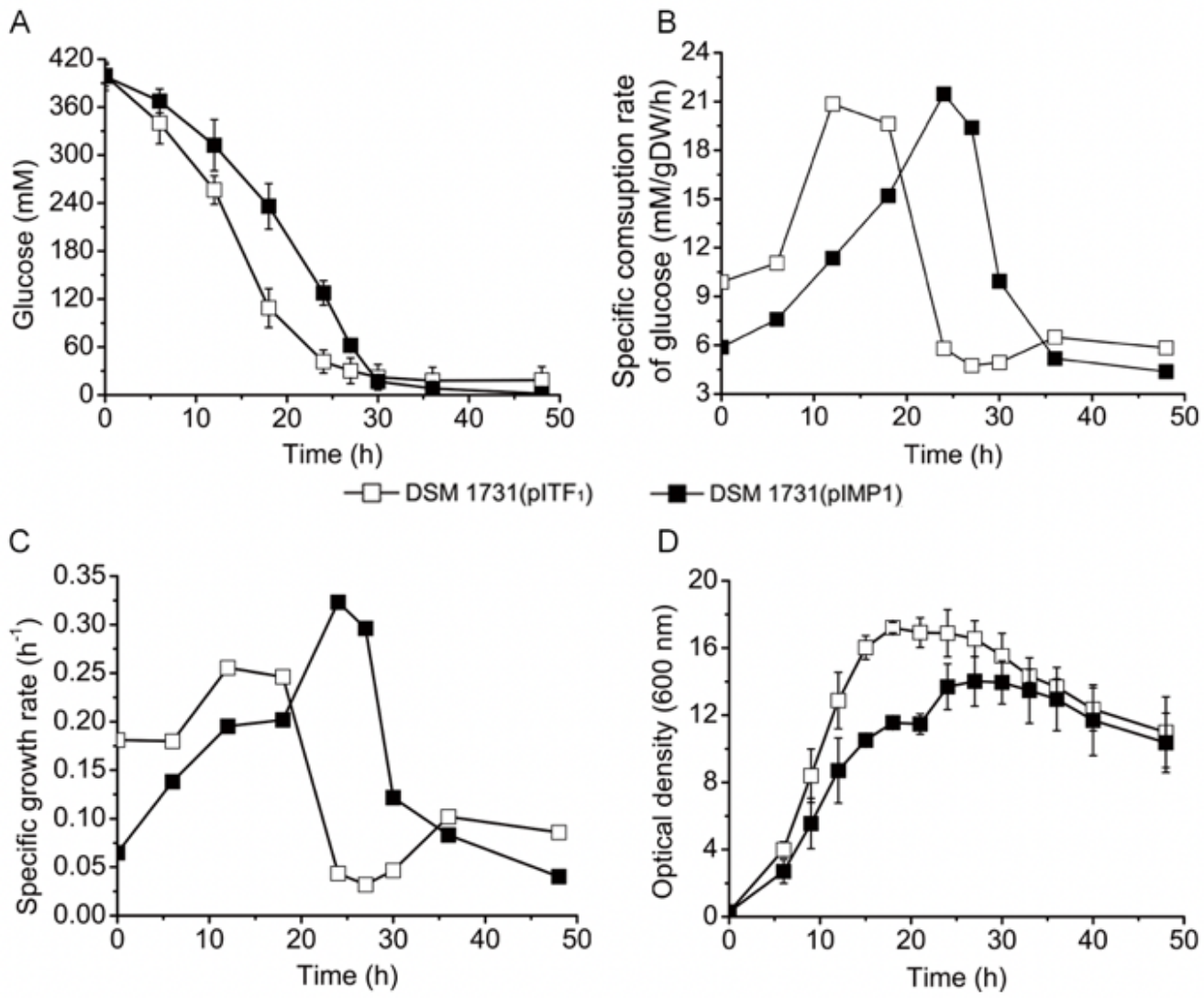

Figure 2

The glucose consumption and cell growth curves of strain DSM1731(pITF1) and strain DSM1731(pIMP1). Glucose utilization (a) and specific rate of glucose consumption (b) profiles of two strains during the 48 hours fermentation. Specific growth rate (c) and cell growth (d) profiles of two strains during the anaerobic fermentation of C. acetobutylicum.

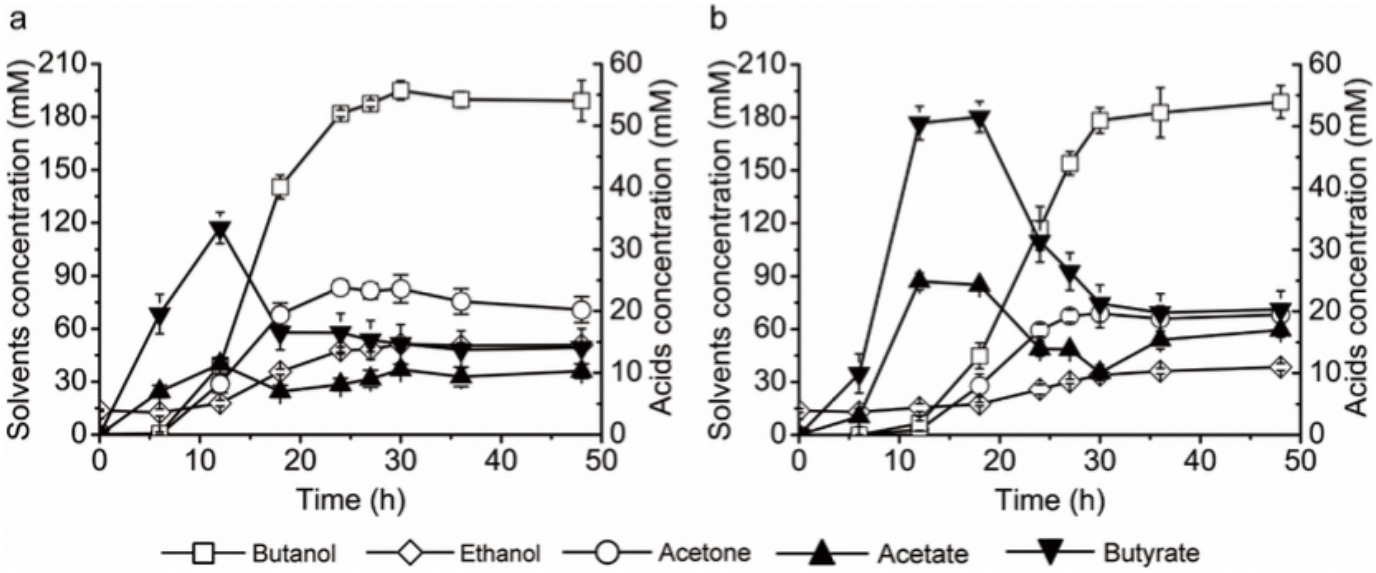

Figure 3

Metabolites production for pH-controlled (pH≥5.0) anaerobic batch fermentations of strain DSM1731(pITF1) and strain DSM1731(pIMP1). (a)Solvent and acid production profiles of strain DSM1731(pITF1). (b) Solvent and acid production profiles of strain DSM1731(pIMP1).

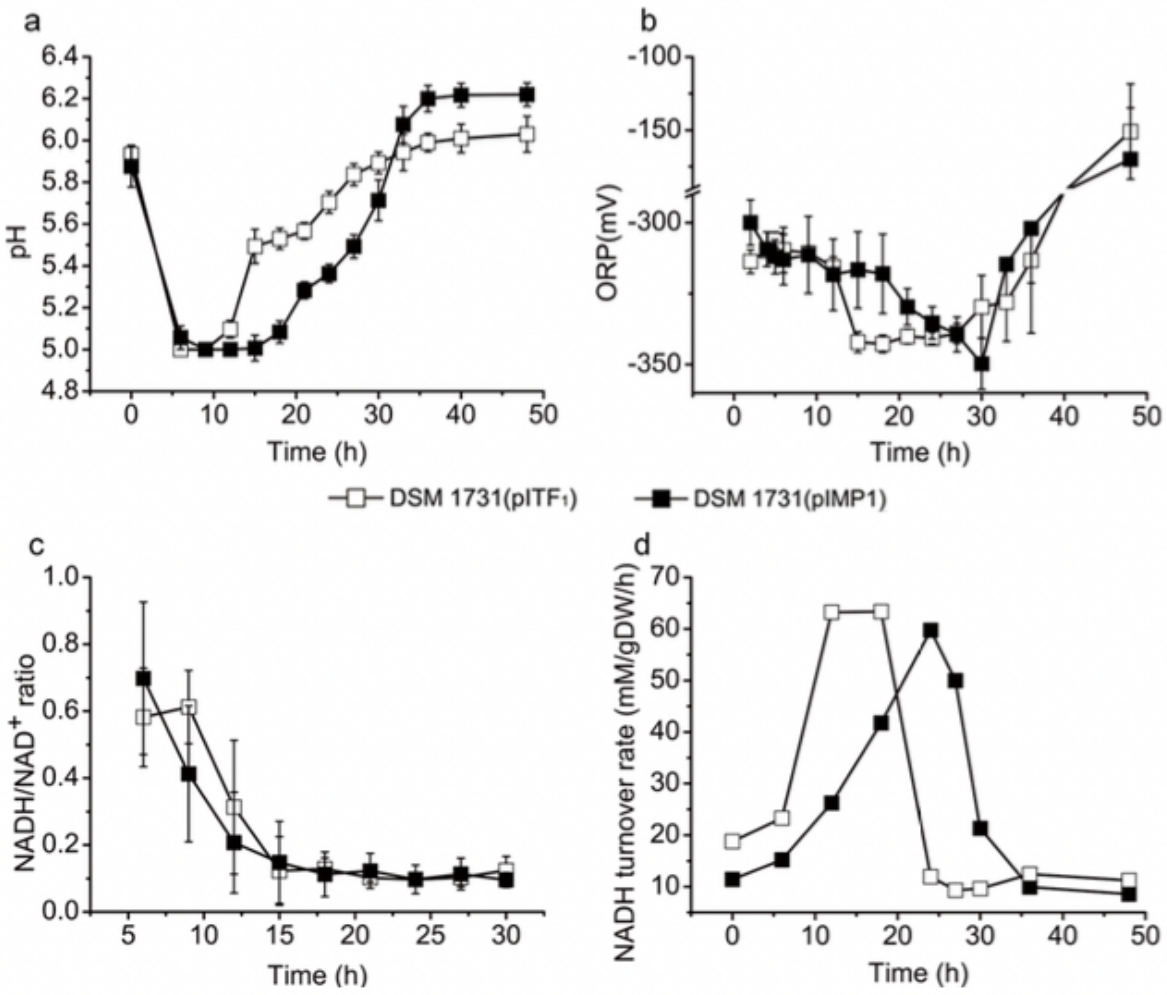

Figure 4

(a)The pH curves of strain DSM1731(pITF1) and strain DSM1731(pIMP1) during 48 hours fermentation. (b) The ORP curves of strain DSM1731(pITF1) and strain DSM1731(pIMP1) during 48 hours fermentation. (c) NADH/NAD+ ratio and (d) NADH turnover rate of strain DSM1731(pITF1) and strain DSM1731(pIMP1).

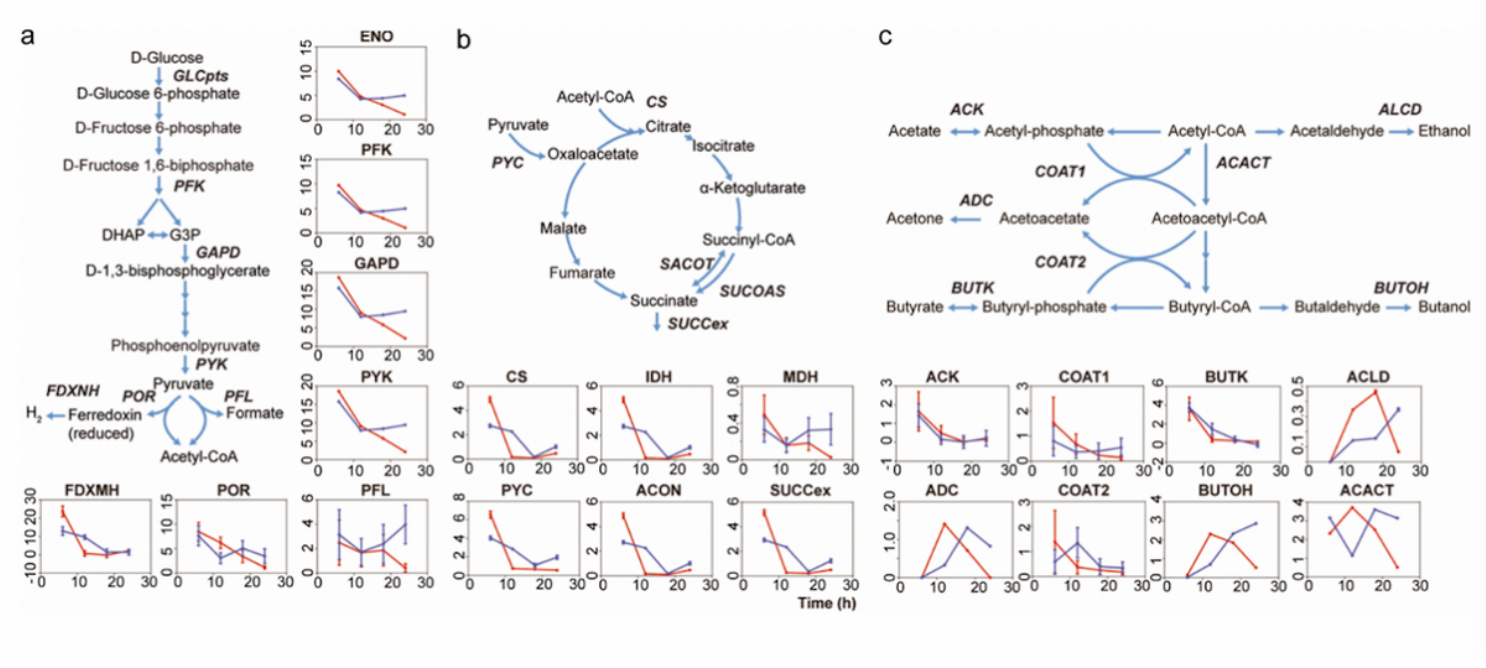

Figure 5

Metabolic flux changes of F1-ATPase overexpression strain 1731(pITF1) compared to its plasmid control strain 1731(pIMP1) in glycolysis (a), TCA cycle (b), and ABE fermentation pathway (c). Red, 1731(pITF1); blue, 1731(pIMP1). X-axis: time (h) and y-axis: flux (mM/gDW/h) were adopt for all the figures. Metabolites: DHAP, dihydroxyacetone phosphate; G3P, D-glyceraldehyde 3-phosphate.

Supplementary Files

This is a list of supplementary files associated with this preprint. Click to download.

- Supplementarytables.xlsx
- TableS1.docx